

J/ ψ production at the STAR experiment

Pavla Federičová for the STAR collaboration^{1,*}

¹Czech Technical University in Prague, Faculty of Nuclear Sciences and Physical Engineering,
Czech Republic

Abstract. The suppression of J/ ψ production in heavy-ion collisions compared to p+p collisions, caused by the color screening in the deconfined medium, has been proposed as a signature of the formation of the Quark-Gluon Plasma. However, J/ ψ production rates are also sensitive to other effects such as the cold nuclear matter effects and recombination. To understand the interplay of these mechanisms, it is important to study J/ ψ production for different collision geometries.

In these proceedings, we present recent result on J/ ψ production via the di-electron decay channel from the STAR experiment at RHIC in p+p collisions at $\sqrt{s_{NN}} = 200, 500$ GeV, in d+Au collisions at $\sqrt{s_{NN}} = 200$ GeV and in heavy-ion collisions, specifically Au+Au collisions at $\sqrt{s_{NN}} = 200$ GeV and U+U collisions at $\sqrt{s_{NN}} = 193$ GeV. We also show measurements on J/ ψ production via the di-muon decay channel in p+p collisions at $\sqrt{s_{NN}} = 500$ GeV and in Au+Au collisions at $\sqrt{s_{NN}} = 200$ GeV using the newly installed Muon Telescope Detector.

1 Introduction

Quarkonium production is one of the essential probes to study the properties of the Quark-Gluon Plasma (QGP) formed in relativistic heavy-ion collisions. J/ ψ is the lightest and most abundantly produced quarkonium state at the STAR experiment. The suppression of its production due to the color-screening effect in the medium has been proposed as a direct evidence of the QGP formation [1].

However, other effects can also affect the observed J/ ψ yields. These effects include firstly Cold Nuclear Matter (CNM) effects such as initial state parton scattering, nuclear shadowing and nuclear absorption, and secondly regeneration via coalescence of deconfined charm quarks. To understand these different mechanisms, it is important to study the quarkonium production in different collision systems and at different collision energies.

The interpretation of medium-induced J/ ψ modification requires a good understanding of its production mechanisms in p+p collisions, which include direct production via gluon fusion, feed-down from higher charmonium states and B-meson decay [2].

The modification of quarkonium production in nucleus+nucleus collisions (A+A) with respect to p+p collisions is usually quantified as the so-called nuclear modification factor (R_{AA}):

$$R_{AA} = \frac{1}{\langle N_{coll} \rangle} \frac{d^2N_{AA}/dp_T dy}{d^2N_{pp}/dp_T dy}. \quad (1)$$

*e-mail: pavla.federicova@fjfi.cvut.cz

It is defined as the ratio of particle yields in A+A collisions to that in p+p collisions scaled by the average number of binary collisions $\langle N_{coll} \rangle$. If there is no medium effect, the production in A+A collisions is a simple superposition of the nucleon-nucleon interactions and R_{AA} is equal to unity. If the production is suppressed (enhanced), then $R_{AA} < 1 (> 1)$.

In these proceedings, we present the measurements of J/ψ production via the di-electron decay channel in p+p collisions at $\sqrt{s_{NN}} = 200, 500$ GeV, in d+Au collisions at $\sqrt{s_{NN}} = 200$ GeV and in heavy-ion collisions, such as Au+Au collisions at $\sqrt{s_{NN}} = 200$ GeV and U+U collisions at $\sqrt{s_{NN}} = 193$ GeV. We also report the first J/ψ measurements via the di-muon decay channel in p+p collisions at $\sqrt{s_{NN}} = 500$ GeV and in Au+Au collisions at $\sqrt{s_{NN}} = 200$ GeV using the newly installed Muon Telescope Detector (MTD) [3].

2 STAR experiment

The STAR experiment is a multi-purpose detector dedicated to the study of the strongly interacting matter at high temperature and high-energy density [4]. Its main purpose is to detect, track and identify charged particles at mid-rapidity. STAR consists of various subsystems which perform different tasks, such as triggering, particle identification or tracking. Enclosed in a 0.5 Tesla solenoidal magnet are a Time Projection Chamber (TPC) [5], a Time-Of-Flight detector (TOF) [6], and a Barrel Electro-Magnetic Calorimeter (BEMC) [7]. The TPC is the main tracking detector for STAR. It also provides particle identification capability through the measurement of specific energy loss (dE/dx). The TOF greatly improves particle identification at low transverse momenta (p_T). The BEMC is used to trigger on and identify high p_T electrons. These detectors cover full azimuth over a large pseudo-rapidity range ($|\eta| < 1$).

In 2014, the MTD [3] was fully installed outside of the solenoidal magnet at STAR. It is designed for triggering on and identifying muons with $p_T > 1.2$ GeV/c at mid-rapidity ($|y| < 0.5$). Compared to the di-electron decay channel, the di-muon decay channel is less affected by bremsstrahlung radiation, Dalitz decay, and γ conversion.

3 J/ψ measurement in p+p collisions

The differential cross section of J/ψ production as a function of p_T has been measured in p+p collisions. Figure 1 shows the STAR results (red circles) using the 2012 data and PHENIX results (black circles) both at $\sqrt{s} = 200$ GeV via the di-electron channel. STAR and PHENIX results are consistent with each other. In figure 2, the results at $\sqrt{s} = 500$ GeV from the di-muon (black circles) and di-electron channels (red circles) for $0 < p_T < 20$ GeV/c are shown. The CGC+NRQCD calculations (low p_T) [8] and NLO NRQCD calculations (high p_T) [9] can together describe the experimental data well both at 200 GeV and 500 GeV.

STAR also studied the dependence of J/ψ production on event activity in p+p collisions at $\sqrt{s} = 200$ GeV and at $\sqrt{s} = 500$ GeV. As can be seen in figure 3, a faster-than-linear growth of relative J/ψ yield versus event activity has been observed, which suggests correlation between soft and hard processes. Such an increase is found to be largely independent of collision energy when comparing the STAR results at $\sqrt{s} = 200$ GeV and at $\sqrt{s} = 500$ GeV with the LHC results at $\sqrt{s} = 7$ TeV [10].

4 J/ψ measurement in d+Au collisions

In order to identify the modification to J/ψ production due to the presence of QGP, all other nuclear effects need to be understood and quantified. CNM effects [11] coming from the presence of ordinary

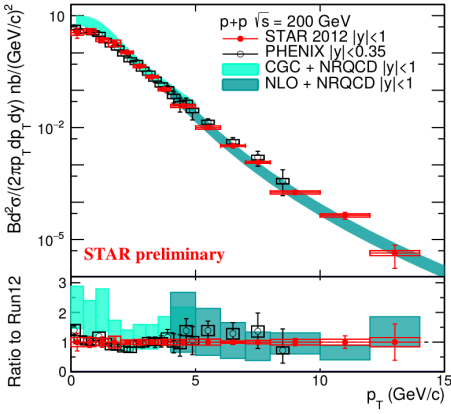


Figure 1. J/ψ production cross section as a function of p_T in $p+p$ collision at $\sqrt{s} = 200$ GeV measured via the di-electron decay channel by the STAR (closed circles) and PHENIX (open circles) experiments.

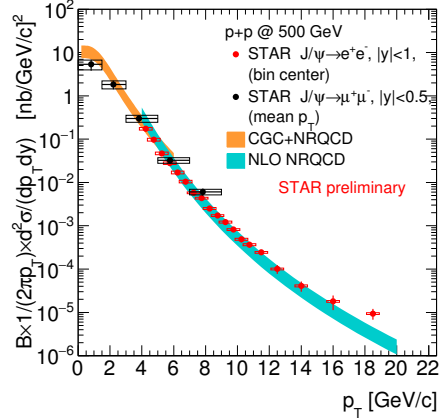


Figure 2. J/ψ cross section as a function of p_T in $p+p$ collision at $\sqrt{s} = 500$ GeV measured via the di-muon decay channel (black circle) and the di-electron decay channel (red circle).

nuclear matter in the collision can modify the production of J/ψ . These effects at RHIC are studied via $d+\text{Au}$ collisions at $\sqrt{s_{NN}} = 200$ GeV where the formation of the QGP is not expected, but nuclear matter is present.

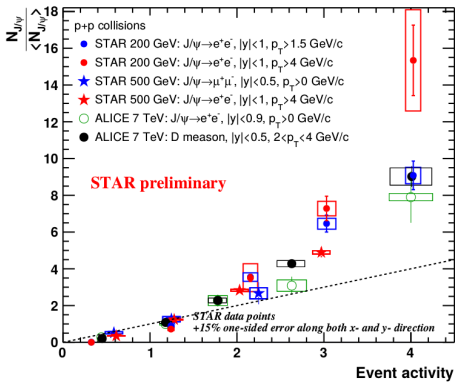


Figure 3. Relative J/ψ yield versus event activity in $p+p$ collisions at $\sqrt{s} = 200$ GeV and $\sqrt{s} = 500$ GeV compared with the LHC results at $\sqrt{s} = 7$ TeV.

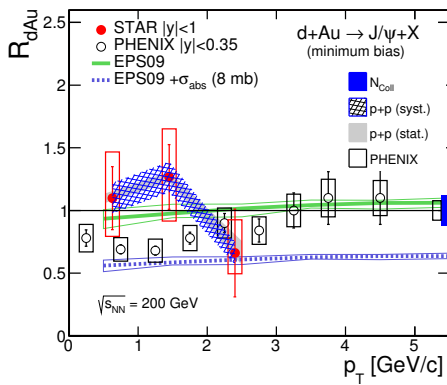


Figure 4. The $\text{J}/\psi R_{AA}$ as a function of p_T in $d+\text{Au}$ collisions (closed circles). The data are compared with PHENIX results (open circles) and EPS09 calculations.

The J/ψ nuclear modification factor measured in $d+\text{Au}$ collisions as a function of p_T is shown in figure 4. The STAR results [12] are compared to the PHENIX data [13] and are in agreement within statistical and systematic uncertainties. The model calculations assuming only shadowing

(EPS09 [14]) as well as shadowing combined with nuclear absorption are also shown and both can qualitatively describe the data. At high p_T , the R_{dAu} is consistent with unity suggesting that the influence of CNM effects is small. At low p_T , the PHENIX results indicate sizeable CNM effects for $p_T < 2$ GeV/c.

5 J/ψ measurement in Au+Au collisions

J/ψ invariant yields in Au+Au collisions at $\sqrt{s_{NN}} = 200$ GeV have been studied via both the di-electron and di-muon channels.

Figure 5 shows the J/ψ nuclear modification factor in the di-electron channel from STAR (solid and open circles) [15] and PHENIX (open squares) [16] as a function of p_T for different collision centralities. The J/ψ suppression decreases towards high p_T for all centralities and is consistent with unity at high p_T in peripheral and semi-peripheral collisions. The data are compared with theoretical predictions including color screening effect and regeneration of charm quarks by Zhao and Rapp (solid line) [17] and Liu et al. (dashed line) [18].

Centrality dependence of the J/ψ nuclear modification factor is shown in figure 6. The STAR data for $p_T < 5$ GeV/c (black circles) [15] and for $p_T > 5$ GeV/c (red circles) [19] indicate J/ψ suppression for central collisions. The suppression increases with collision centrality. The high p_T J/ψ mesons are less suppressed than the low p_T ones, which could be due to the less influence of recombination and CNM effects at high p_T . Theoretical models by Zhao and Rapp (solid line) [17] and Liu et al. (dashed line) [18] can qualitatively describe the data.

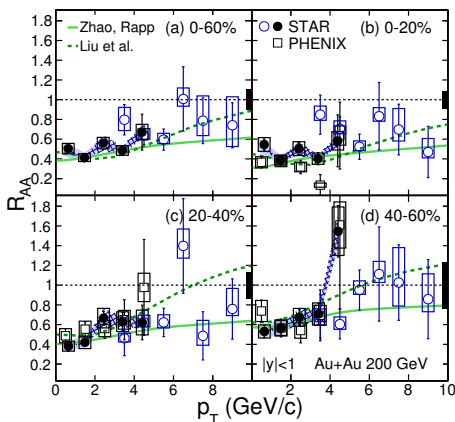


Figure 5. The J/ψ nuclear modification factor as a function of p_T for different centralities in Au+Au collisions.

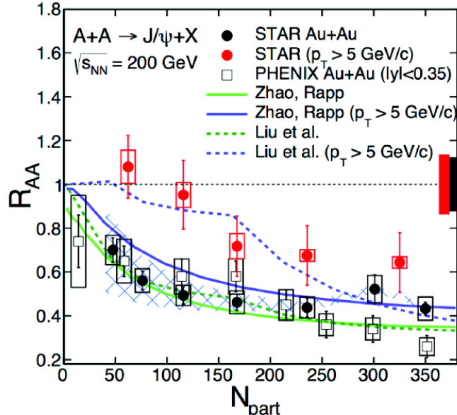


Figure 6. The J/ψ nuclear modification factor as a function of centrality for the STAR low (black circles) and high p_T data (red circles).

Figure 7 shows the invariant yield of J/ψ from the di-muon channel (solid points) as a function of p_T for different collision centralities. These new results are consistent with the STAR published results from the di-electron decay channel (open points) [20, 21] within uncertainties.

Centrality dependence of J/ψ R_{AA} from the MTD data (red stars) is shown in figure 8 for $p_T > 0$ GeV/c and in figure 9 for $p_T > 5$ GeV/c. Results from PHENIX in Au+Au collisions at $\sqrt{s_{NN}} = 200$ GeV (black open circles) [16], as well as results from ALICE [22] and CMS [23] in

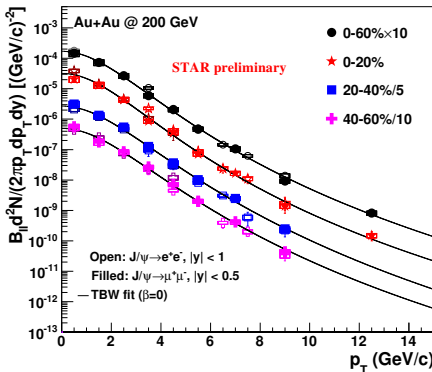


Figure 7. The J/ψ invariant yield as a function of p_T for different centralities in the di-muon decay channel (solid points) and in the di-electron decay channel (open points).

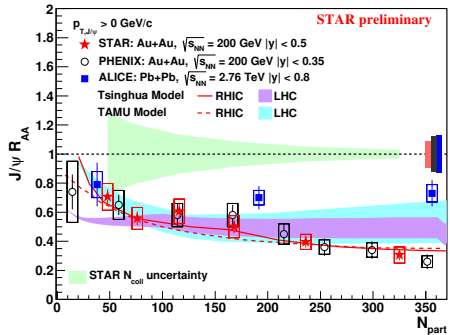


Figure 8. The J/ψ nuclear modification factor for $p_T > 0$ GeV/c in Au+Au collisions at $\sqrt{s_{NN}} = 200$ GeV and in Pb+Pb collisions at $\sqrt{s_{NN}} = 2.76$ TeV as a function of centrality.

Pb+Pb collisions at $\sqrt{s_{NN}} = 2.76$ TeV (blue solid circles) are shown in figure 8 and figure 9, respectively. For $p_T > 0$ GeV/c, the STAR results are consistent with the PHENIX results, both of which decrease with increasing centrality, while the ALICE results are almost independent of centrality and less suppressed than those at RHIC in central collisions. Such a difference can be explained by larger regeneration contributions to the low p_T J/ψ at the LHC due to higher $c\bar{c}$ yields. Both transport models from Tsinghua [18, 24] and Texas A&M University (TAMU) [17, 25], including dissociation and regeneration effects, can qualitatively describe the centrality dependence at RHIC, but tend to overestimate the suppression at the LHC.

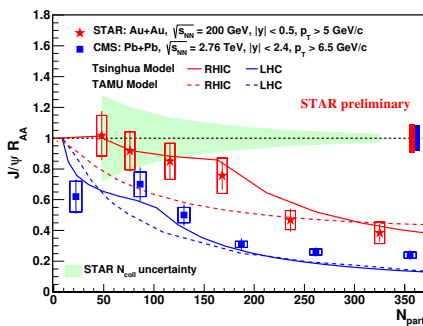


Figure 9. The J/ψ nuclear modification factor for $p_T > 5$ GeV/c in Au+Au collisions at $\sqrt{s_{NN}} = 200$ GeV and in Pb+Pb collisions at $\sqrt{s_{NN}} = 2.76$ TeV as a function of centrality.

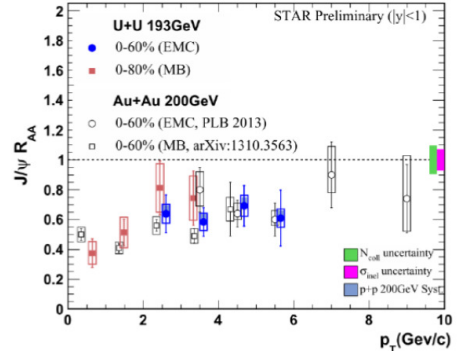


Figure 10. The J/ψ nuclear modification factor as a function of p_T in U+U collisions at $\sqrt{s_{NN}} = 193$ GeV compared with Au+Au collisions at $\sqrt{s_{NN}} = 200$ GeV.

For $p_T > 5$ GeV/c, the R_{AA} both at RHIC and the LHC have a decreasing trend towards the central collisions, but RHIC data exhibit less suppression than that at the LHC in all centralities. This is

expected due to higher energy density and temperature reached at the LHC, leading to stronger J/ψ suppression. At high p_T , there is a tension among the transport models and experimental data.

6 J/ψ measurement in U+U collisions

STAR has also collected data for U+U collisions at $\sqrt{s_{NN}} = 193$ GeV. Since uranium nuclei are larger than gold nuclei, it is expected that the energy density of the medium created in U+U collisions is higher than that in Au+Au collisions [26].

Figure 10 shows the STAR results on J/ψ nuclear modification factor in U+U collisions as a function of p_T . The suppression of J/ψ production is similar to that observed in Au+Au collisions at $\sqrt{s_{NN}} = 200$ GeV [27].

7 Summary

We present the J/ψ measurements in the di-electron and the di-muon decay channels at STAR. In p+p collisions at $\sqrt{s} = 200$ GeV and 500 GeV, inclusive J/ψ cross section can be described by CGC+NRQCD and NLO NRQCD model calculations. The modification of J/ψ production in d+Au collisions at $\sqrt{s_{NN}} = 200$ GeV is consistent with no suppression at high p_T suggesting no CNM effects but indicating sizeable CNM effects at low p_T .

In Au+Au collisions at $\sqrt{s_{NN}} = 200$ GeV, we observe clear evidence of J/ψ suppression indicating dissociation. The J/ψ R_{AA} can be qualitatively described by theoretical models including dissociation and regeneration. Suppression of J/ψ production in U+U collisions at $\sqrt{s_{NN}} = 193$ GeV is similar to that observed in Au+Au collisions at $\sqrt{s_{NN}} = 200$ GeV.

Acknowledgement

This work was supported by the grant No. 13-20841S of Grant Agency of the Czech Republic.

References

- [1] T. Matsui and H. Satz, Phys.Lett. B **178**, 416-422 (1986)
- [2] N. Brambilla et al., Eur. Phys. J. C **71**, 1534 (2011)
- [3] L. Ruan et al., J. Phys. G: Nucl. Part. Phys. **36**, 095001 (2009)
- [4] K. Ackermann et al. (STAR Collaboration), Nucl.Instrum.Meth. A **499**, 624-632 (2003)
- [5] M. Anderson, J. Berkovitz, W. Betts, R. Bossingham, F. Bieser, et al., Nucl.Instrum.Meth. A **499**, 659-678 (2003)
- [6] W. Llope (STAR Collaboration), Nucl.Instrum.Meth. A **661**, 110-113 (2012)
- [7] M. Beddo (STAR Collaboration), Nucl.Instrum.Meth. A **499**, 725-739 (2003)
- [8] Y.-Q. Ma, and R. Venugopalan, Phys. Rev. Lett. **113**, 192301 (2014)
- [9] H. Shao et al., JHEP **05**, 103 (2015)
- [10] J. Adam et al. (ALICE collaboration), J. High Energy Physics **09**, 148 (2015)
- [11] R. Vogt, Phys. Rev. C **71**, 054902 (2005)
- [12] L. Adamczyk et al. (STAR Collaboration), Phys. Rev. C **93**, 64904 (2016)
- [13] A. Adare et al. (PHENIX Collaboration), Phys. Rev. C **87**, 034904 (2013)
- [14] K. Eskola, H. Paukkunen, and C. Salgado, Nucl. Phys. A **830**, 599 (2009)
- [15] L. Adamczyk et al. (STAR Collaboration), Phys. Rev. C **90**, 24906 (2014)

- [16] A. Adare et al. (PHENIX Collaboration), Phys. Rev. Lett. **98**, 232301 (2007)
- [17] X. Zhao and R. Rapp, Phys. Rev. C **82**, 064905 (2010)
- [18] Y. Liu, Z. Qu, N. Xu, and P. Zhuang, Phys. Lett. B **678**, 72-76 (2009)
- [19] L. Adamczyk et al. (STAR Collaboration), Phys. Lett. B **722**, 55 (2013)
- [20] L. Adamczyk et al. (STAR Collaboration), Phys. Let. B **722**, 55-62 (2013)
- [21] L. Adamczyk et al. (STAR Collaboration), Phys. Rev. C **90**, 024906 (2014)
- [22] B. Abelev et al. (ALICE Collaboration), Phys. Let. B **734**, 314-327 (2014)
- [23] S. Chatrchyan et al. (CMS Collaboration), JHEP **05**, 063 (2012)
- [24] K. Zhou et al., Phys. Rev. C **89**, 054911 (2014)
- [25] X. Zhao and R. Rapp, Nucl. Phys. A **859**, 114-125 (2011)
- [26] D. Kikola, G. Odyniec, and R. Vogt, Phys. Rev. C **84**, 054907 (2011)
- [27] W.M. Zha (STAR Collaboration), Nuclear Physics A **931**, 596-600 (2014)